International Journal of Theoretical Physics, Vol. 37, No. 10, 1998

Dynamics of Olivary Neurons

Gin McCollum[1]

Received January 10, 1996

Excitation of ensembles of climbing fibers—the axons of olivary neurons—in the cerebellum is predicted on the basis of observations of climbing fiber tactile receptive fields. Each stimulus excites an ensemble of climbing fibers, called its image. When receptive fields are eliminated by inhibition, injury, or the functional state of the circuit, the image poset can change. Four maps are explored: the map from the poset of all simultaneous stimulus arrays to the poset of excited ensembles, a map in the reverse direction, the map from the poset of all stimulus sequences of a given number to ensemble response, and a map in the reverse direction. The map from excitation to response is complicated by the oscillatory tendency of climbing fibers, by both phasing and response spike number. The central question motivating the study is to what extent climbing fiber activity allows discrimination of stimuli, either in simultaneous arrays or in sequences of arrays. The question is addressed by predicting equivalence classes, first on the basis of excitation of cells in the inferior olive and then on the basis of response in the climbing fibers to which they give rise. The paper provides a mechanism for climbing fibers to behave as event detectors, assuming an oscillatory behavior of inferior olive cells. It also provides another example of the combination of continuous and discrete aspects of nervous system function.

1. INTRODUCTION

The nervous system uses a variety of organizations to transform sensory information for combination with other sensory information or for motor use. In some systems, the information is transformed using a neighbor-preserving mapping (Schwartz, 1977). That is not true among the tactile responses of climbing fibers, the axons of olivary neurons, which powerfully activate Purkinje cells in the cerebellum (Fig. 1). In order to analyze their organization of cerebellar climbing-fiber tactile receptive fields, we have taken an approach McIlwain (1986) calls "point image": the ensemble response to a single

[1] Neurological Sciences Institute, Oregon Health Sciences University, 1120 NW 20th Ave., Portland, Oregon 97209, mccollum@ohsu.edu

0020-7748/98/1000-262 7$15.00/0

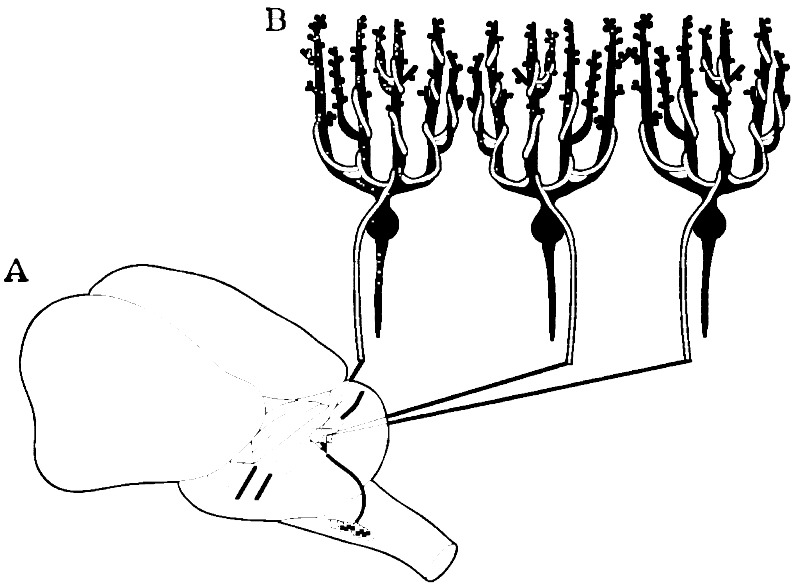

Fig. 1. Sketch of a cat's brain, with an enlargement of climbing fibers entwining Purkinje cells. (A) A cat's brain as viewed from above, behind, and to the left. The lobes of the cerebral cortex are the two large, smooth lobes at the left of the figure (front of the cat). Just behind the cerebral cortex, and a little under its edge, is the cerebellar cortex, which forms a roof over the other parts of the cerebellum, such as the cerebellar nuclei, which are not shown. The cerebellar cortex is folded in fine lateral folds, because, if spread out, it would be much longer from front to back than from side to side. (Also the human cerebellar cortex is more finely folded than the cerebral cortex.) Leading from under the cerebellar cortex and off to the right is the brain stem. Within the brain stem, the inferior (meaning lower in the brain stem) olivary nucleus (commonly called the inferior olive) is identified by dotting. Each climbing fiber arises from a neuron in the inferior olive and goes to the cerebral cortex, as indicated by the heavy line. In the cerebellar cortex (as indicated by the small rectangle), each Purkinje cell receives exactly one climbing fiber, although each olivary cell sends climbing fibers to about 10 Purkinje cells. (B) Purkinje cells entwined by climbing fibers. The black neurons are Purkinje cells, the largest cells in the cerebellum and the only output cells. Purkinje cells are arrayed on a 2-surface like a field of radishes, with their dendrites (the top part, where the radish leaves would be) remaining close to a plane perpendicular to the surface of the cerebellar cortex and parallel to the front–back axis of the cat. The axon (output) is down (radish root); the dendrite is for input and perhaps input transformation. The white fibers are climbing fibers. Each one wraps around its Purkinje cell, synapsing many times. If the climbing fiber spikes, so does the Purkinje cell. In contrast, the other major input to the Purkinje cells, the parallel fibers, rely on large numbers and small influence per fiber. Each Purkinje cell can receive 100,000–200,000 parallel fiber synapses.

stimulus (McCollum and Robertson, 1988; McCollum, 1992; Castelfranco *et al.*, 1994). The first part of this paper formalizes previous work on spatial aspects of climbing fiber response (Section 2) in such a way that it can be combined with experimental results on temporal aspects to yield spatiotemporal mapping (Section 3). Spatiotemporal mapping can be used to understand how two sets of apparently conflicting experimental results—one set indicating that climbing fibers fire rarely and only in response to unusual or unexpected events and another set indicating that they fire in an ongoing rhythm based on fundamental cellular properties—can arise from similar mappings at different frequencies.

The areas of skin to which cerebellar climbing fibers are sensitive show a surprising orderliness, which can provide focus for studying their collective behavior. The tactile *receptive field* of a particular neuron, such as a climbing fiber, is the area of skin within which a stimulus excites that neuron. The configurations of most cerebellar climbing-fiber tactile receptive fields can be generated by means of a few rules. The two major rules are iterative, so that the total set of possible configurations is highly regular (McCollum, 1992). Under the assumption that total excitation among a collection of climbing fibers is simply the union of individual excitations, the full set of configurations can be used to predict the ensembles that respond to spatially and temporally complex stimuli.

Ensembles of climbing fibers can distinguish more locations on the skin than one climbing fiber, but their spatial resolution is limited to that of the intersections of receptive fields. Among the climbing fibers, receptive field boundaries have segments in common, so that it is meaningful to determine the minimal areas of skin that are intersections of or differences of receptive fields (McCollum and Robertson, 1988) (Fig. 2). A *compartment* is a minimal (under set-theoretic inclusion) nonempty Boolean combination of receptive fields, in the sense that no other nonempty Boolean combination of receptive fields is properly contained within it. Because these definitions are based on observations of climbing fibers, "receptive field" and "compartment" will refer to those of cerebellar climbing fibers for the remainder of the paper. However, the results in the paper may generalize to other cell populations. Compartments are the smallest skin areas that ensembles of climbing fibers can distinguish. This quantization of areas allow for a discrete analysis of structure to which continuous or differentiable analyses would be oblivious.

Because the set of receptive fields is finite, each receptive field is a union of compartments. Only particular combinations of compartments have been observed to occur together in unions as receptive fields (McCollum, 1992). The rules generating receptive fields from compartments are given in Section 2.

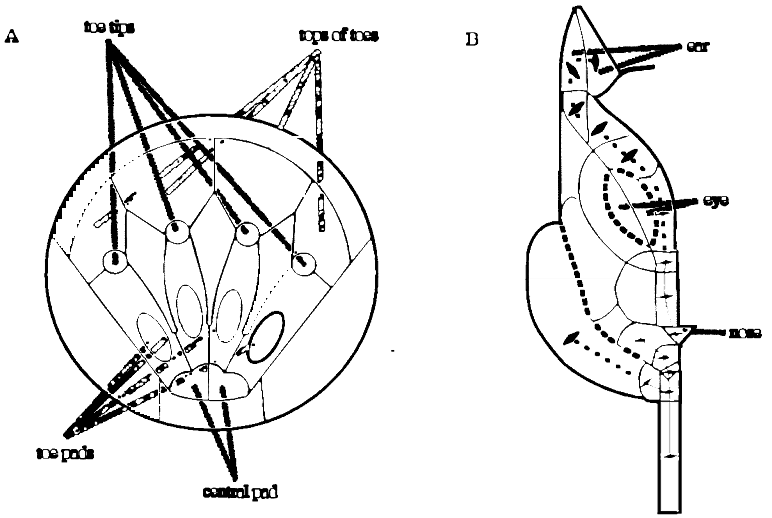

Fig. 2. Diagrams showing anterior lobe compartments on the cat hindpaw and face, and CF-contiguity on the face. These are static diagrams, or skeletal pictures, of a sort of grid of the cat's paw and face, as represented among the cerebellar climbing fibers. (A) Hindpaw. The lines are boundaries or boundary segments of receptive fields. The empty spaces are the compartments, or minimal Boolean combinations of sets of receptive fields. The top, bottom, and sides of the paw are projected onto the plane. The four circular compartments are the toe tips. The areas above them on the page are the backs (tops) of the toes. The elongated diamond-shaped areas between the toe tips are the skin between the toes. The four ovals, one below each toe tip, are the toe pads. The central pad, with three humps, is divided in the middle. This is a simplified diagram; more detail can be found in McCollum (1992). (B) Face. The diagram shows the right half of the cat's face, with the ear at the top, the nose crossing the midline, and the smallest compartment the lower lip. The strip at the bottom goes under the chin. The lateral bulge is under the jaw. There is a dashed line at the jaw line. Thick solid lines and dashed lines indicate compartment boundaries. Dashed lines are not crossed by receptive fields. Thin solid lines and dotted lines indicate binary CF-contiguity between compartments marked with diamonds. Compartments not connected by binary CF-contiguity are included in receptive fields, but not enough such receptive fields have been observed to induce rules for generating them. More detail on face compartments and binary CF-contiguity can be found in Castelfranco, *et al.* (1994).

Previous papers have organized the experimental data of Robertson and colleagues to allow formalization (McCollum and Robertson, 1988; McCollum, 1992; Castelfranco *et al.*, 1994). Definitions and assumptions used in this paper are developed in the previous ones, but stated more formally here. The assumptions cover all but a few of the observed cases of paw receptive fields reported by Robertson and colleagues, and have predicted receptive field types found in later experimental studies (McCollum, 1992).

Because of the controversy surrounding the temporal and situational behavior of climbing fibers (Simpson *et al.*, 1996), this paper is divided into

a purely spatial part (Section 2), based on the results of Robertson and colleagues, and a temporal part (Section 3), based on the results of Llinás and colleagues. Even though the work of Llinás and colleagues indicates deterministic responses of climbing fibers according to resetting of their internal rhythms by previous stimulation, it could be argued that there is a stochastic component to the response pattern. However, neither such a stochasticity nor the controversy over which stimulus patterns lead to responses affects the conclusion by Robertson and colleagues that the receptive fields for light, punctate stimuli are discrete.

The purpose of this paper is to present the patterns of response among climbing fibers, given a range of tactile stimuli. The ability of the climbing fiber responses to discriminate stimuli has been questioned because of the climbing fibers' low firing frequency and large receptive fields. Specification of response patterns allows determination of equivalence classes of stimuli—those that evoke responses in the same climbing fibers in the same patterns—and the climbing fibers' ability to discriminate stimuli. This paper will only consider cell activity caused by external stimulation, even though the activity of ensembles of climbing fibers is affected by both cellular and circuit interactions. Spatially and temporally distributed stimulus arrays will be constricted by combining single-compartment stimuli used in experiments (Rushmer *et al.*, 1980; Robertson, 1987; Robertson and Elias, 1988; Castelfranco *et al.*, 1994). The assumption will be made that the simultaneous stimulation of more than one compartment does not change the receptive field of any given cell. The ensemble response indicated by single-neuron receptive fields can then be used as a background against which cellular and circuit interaction effects can be seen as perturbations.

2. ONE-TIME SPATIALLY DISTRIBUTED STIMULUS ARRAY

The set of available receptive fields limits the stimulus arrays that can be distinguished. In the case of discrete compartments, receptive fields limit the discrete excitation patterns that occur. Distinct stimulus arrays can evoke the same excitation pattern, so that the stimulus arrays are "excitation-equivalent." [In previous publications, we have used the term "response-equivalence" (Robertson and McCollum, 1989, 1991). In this paper, the consideration of subthreshold oscillation is added in later sections; the term "response-equivalence" is reserved until then.] This section will present the receptive fields in the anterior lobe, the more limited set of receptive fields in the paramedian lobule, the excitation mapping for general receptive fields of this type, and the effects of lesions described by eliminating receptive fields.

In this section, the whole stimulus is assumed to arrive at the same instant: it can be spatially, but not temporally distributed. Because stimuli

within the same compartment excite the same set of climbing fibers, there is no loss of generality in fixing for each compartment i a nonempty set $*_i$ of point stimuli arriving simultaneously within compartment i; $*_i$ will be referred to as a "single-compartment stimulus." Any stimulus to skin included in one or more compartments can be specified as a union of single-compartment stimuli $\cup_{i \in I} *_i$, where I is a subset of the set of compartments; such a multicompartment stimulus will be called a "stimulus array" for emphasis.

2.1. Receptive Fields in the Anterior Lobe

Most of the combinations of compartments that form paw or face receptive fields in the anterior lobe are specified by three generative rules. Descriptions of receptive fields are minor idealizations from experimental observation: a few paw receptive fields require a further generative rule, and on some parts of the body there are not enough observed receptive fields to be sure of their organization (McCollum, 1992; McCollum and Robertson, 1988; Castelfranco *et al.*, 1994). [For more completeness, including clumps, see McCollum (1992).] Toe compartments combine in a way that is sensitive to anatomical equivalence between skin areas; for example, toe pads are anatomically equivalent to each other. Non-toe compartments combine according to binary relations analogous to contiguity on the skin.

The generative rules are based on two types of symmetric relations between compartments, analogous to contiguity on the skin. One is binary *CF-contiguity* (CF for climbing fiber) between pairs of compartments (McCollum, 1992). (Contiguity is between compartments rather than climbing fibers.) The generative rule using this relation is:

Rule 1: If compartment c_1 is included in a receptive field r_1, and compartment c_2 is binary CF-contiguous with c_1, then $r_1 \cup c_2$ is also a receptive field.

Rule 1 governs almost all face receptive fields (McCollum, 1992; Castelfranco *et al.*, 1994). Also, it governs the compartments on the paws not associated with particular toes, like the central pad and the compartments at the sides of the paws.

Rules 1 and 2 are in iterative form and so require a seed, or first compartment in a receptive field. Among the face and paw receptive fields analyzed so far (McCollum, 1992; Castelfranco *et al.*, 1994), not all compartments occur separately as receptive fields and, to form the observed receptive fields, not all compartments are required as seeds. Rule 3 will be stated before Rule 2.

Rule 3: There is a nonempty subset of compartments, each of which is a receptive field.

Paw compartments combine according to *toe CF-contiguity*, a binary, symmetric relation between pairs of toes and between pairs of anatomical equivalence classes across toes. Only neighboring toes are toe CF-contiguous. Toe CF-contiguity between anatomical equivalence classes is more complicated, because they are not sequential (McCollum, 1992). In iterative form, the rule applying to toes is:

Rule 2: Let receptive field r consist exactly of elements of anatomical equivalence classes $L_1, \ldots, L_m$ on toes $\mu_1, \ldots, \mu_n$. If anatomical equivalence class N is toe CF-contiguous to any in the set $L_1, \ldots, L_m$, then there exists a receptive field consisting of the union of r with the elements of N on toes $\mu_1, \ldots, \mu_n$. There also exists a receptive field consisting of the union of r with the elements of $L_1, \ldots, L_m$ on toe k if toe k is a neighbor to any of the toes $\mu_1, \ldots, \mu_n$.

Rule 2 results in receptive fields that include only anatomically equivalent areas on the toes involved in the receptive field (a property called "rectangularity" in McCollum, 1992). If the iterative Rules 1 and 2 accurately reflect the processes by which receptive fields are formed, one would expect rare nonrectangular receptive fields to be formed by a combination of Rules 1 and 2.

When the receptive fields generated by the rules of combination are arranged as posets (Fig. 3), it is easy to specify excitation. If receptive field r_1 includes receptive field r_2, then every time cells with receptive field r_2 are excited by a stimulus, so are the cells with receptive field r_1.

Rule 2 generates a set of receptive fields that can be organized into triangular subposets. Given a sequentially labeled set of pairwise CF-contiguous compartments $C = \{c_1, c_2, \ldots, c_p\}$, let the neighbor set N_p be

$$\{\cup_{i=m}^{n} c_i \colon 1 \leq m \leq n \leq p\}$$

Then the set of all possible receptive fields over any anatomical equivalence class of compartments on the paw is isomorphic to the neighbor set over the four toe pads, N_4 (Fig. 4). The same is true of anatomically equivalent receptive fields, each of which consists of a sequence of compartments along one toe. If one such receptive field F includes another, G, then the neighbor set N_F, associated with F includes the neighbor set N_G, in the sense that each element of N_F includes the corresponding element of N_G (Fig. 4).

The rules of combination bear on the excitation of climbing fibers, because they have implications for the organization of images. For example, we can adduce some consequences of the neighbor rule (Rule 1) on images, for any number z of compartments. The form of the ordered set of images A_i ensemble responses to stimuli $*_i$ is constrained by the fact that receptive fields consist only of groups of neighboring compartments. Suppose that, for

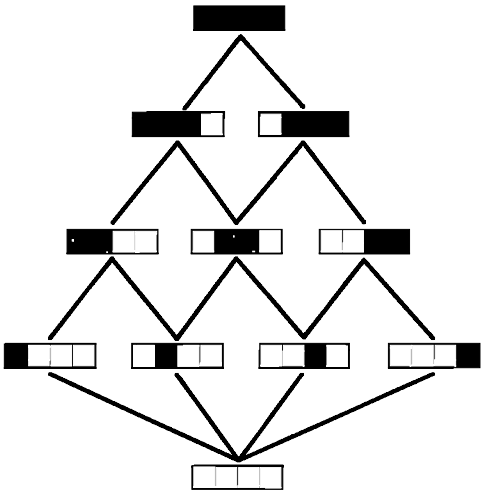

Fig. 3. The poset of toe pad receptive fields for cells in the anterior lobe is the neighbor set. It omits some of the combinations found in the set of possible stimulus arrays. The four toe pad compartments are represented as four contiguous squares. A compartment is shaded if it is included in a receptive field. The join of two receptive fields r_1 and r_2, found in the usual way in the poset, is the minimal receptive field r_3 such that, if cells with receptive fields r_1 or r_2 are excited, so are cells with receptive field r_3.

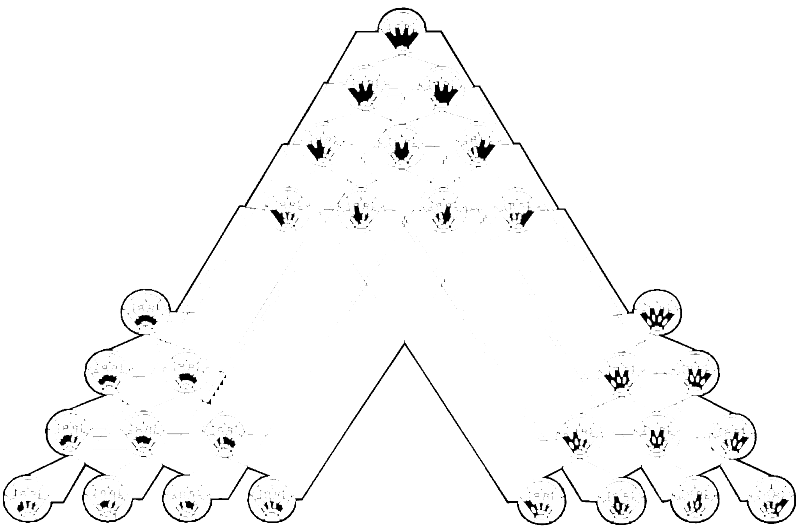

Fig. 4. Example of domination of neighbor-set triangular posets: toe pads and the volar (bottom) surfaces of the toes. Each receptive field is drawn on a paw diagram like the one in Fig. 2A. At the lower left is the triangular subposet of toepads. At the lower right is the triangular subposet of hairy areas around the toepads. At the top is the triangular sub-poset combining toepads with their hairy surrounds.

a particular set of cells with such receptive fields, $A_i > A_j$, where $i, j \in \{1, \ldots, z\}$, $i \neq j$. Then any receptive field that includes compartment j also includes compartment i. If i and j are not neighbors, then any receptive field including compartment j also includes any intervening compartment k. Therefore, $A_k > A_j$. These are general statements, applying to a neighbor set over any number of elements.

Given any set of receptive fields over four compartments labeled sequentially 1 through 4, it is easy to list the specific consequences of the general consequences of the neighbor rule given in the preceding paragraph:

$$A_3 > A_1 \Rightarrow A_2 > A_1$$

$$A_4 > A_1 \Rightarrow A_2 > A_1 \quad \text{and} \quad A_3 > A_1$$

$$A_4 > A_2 \Rightarrow A_3 > A_2$$

$$A_2 > A_4 \Rightarrow A_3 > A_4$$

$$A_1 > A_4 \Rightarrow A_3 > A_4 \quad \text{and} \quad A_2 > A_4$$

$$A_1 > A_3 \Rightarrow A_2 > A_3$$

These statements are true for any set of receptive fields obeying the neighbor rule (rule 1) over four sequentially labeled compartments, and are not drawn specifically from any part of the cerebellum.

2.2 Anterior Lobe versus Paramedian Lobule

The paramedian lobule has a more limited set of receptive fields than the anterior lobe, even though the receptive fields in the paramedian lobule follow the same rules of combination (Fig. 5). Therefore, stimulus arrays are excitation-equivalent in the paramedian lobule that are not in the anterior lobe.

For example, let the set of all stimulus arrays to the toe pads—isomorphic to the power set over the compartments—be mapped onto the set of receptive fields they excite. The anterior lobe distinguishes all stimulus arrays, because each toe pad has an image—set of excited cells—that is not dominated by the image of any other toe pad. When the image of one toe pad T dominates that of another toe pad U, stimulating T masks whether U has been stimulated: stimulating U does not change the pattern of excitation.

Every single-toe-pad image in the paramedian lobule either dominates another or is dominated by another (Fig. 6). For example, A_3 and A_4 dominate other images, but are not dominated by any. A stimulus array $*_3 \cup *_4$ to toe pads 3 and 4 would excite the image union $A_3 \cup A_4$. In contrast, A_3 dominates A_2. The stimulus array $*_3 \cup *_2$ excites $A_3 \cup A_2 = A_3$. In the paramedian lobule, $*_3 \cup *_2$ is excitation-equivalent to $*_3$; they are not excitation-equivalent in the anterior lobe, with its larger set of receptive fields.

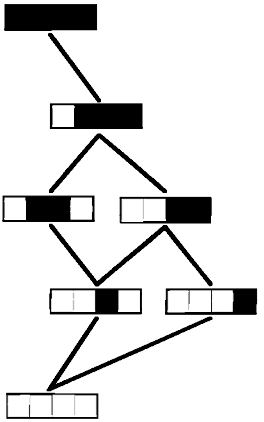

Fig. 5. The poset of toe pad receptive fields found in the paramedian lobule (PML) is a subset of the neighbor set. Toes are drawn as squares rather than in the context of the rest of the paw, for diagrammatic simplicity. Otherwise, the conventions of the poset and the arrangement of the receptive fields in the poset are as in Fig. 4.

The 16 possible stimulus arrays on four toes are divided into seven excitation-equivalence classes by the limited set of receptive fields in the paramedian lobule (Fig. 7). Each excitation-equivalence class is associated with one or two dominant single-toe images, the images whose union is excited by any stimulus array in the excitation-equivalence class. For example, the excitation-equivalence class associated with A_2 is $\{*_2, *_2 \cup *_1\}$: the paramedian lobule does not distinguish whether $*_1$ is included, because A_2 dominates A_1. There is also an excitation-equivalence class associated with A_2 and A_4, neither of which dominates the other. They both dominate A_1; it can be included or not. The excitation-equivalence class associated with A_3 has more elements, because A_3 dominates two images. In that excitation-equivalence class, $*_3$ can be joined with either, neither, or both of $*_1$ and $*_2$.

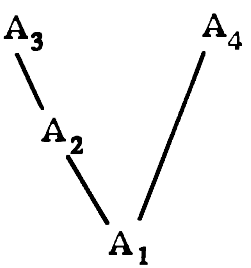

Fig. 6. The poset of images of toe pads found in the paramedian lobule, as deduced from the set of receptive fields (Fig. 5). Each image A_μ is the set of receptive fields excited by stimulation of compartment μ. Only A_3 and A_4 fail to be dominated by other images. A_2 is dominated by A_3, and A_1 is dominated by all the other three images.

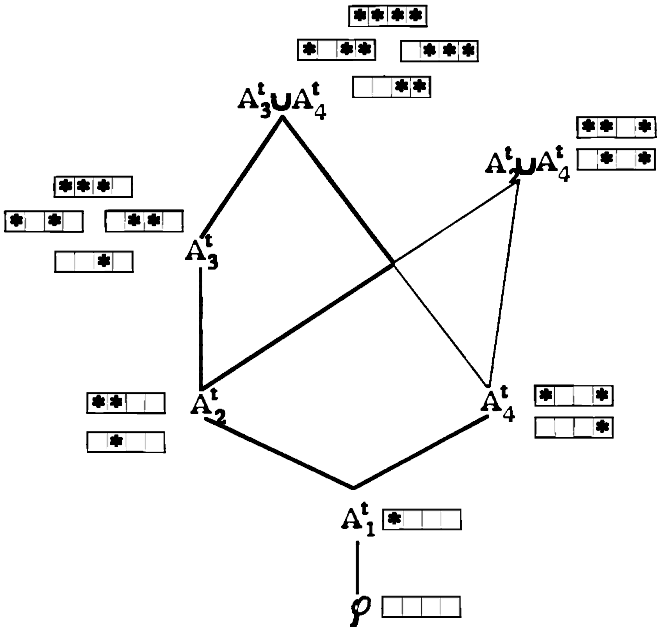

Fig. 7. Poset of ensembles excited by four-compartment stimulus arrays in the paramedian lobule, with excitation-equivalence classes grouped near the ensembles they excite. The excited ensembles are denoted by images and unions of images A_μ. The stimuli are denoted as asterisks.

Similarly, each other excitation-equivalence class is generated in one of two ways, one way being to (1) choose two images A_μ and A_ν, neither of which dominates the other, (2) find the set $\{A_{\kappa(1)}, \ldots, A_{\kappa(n)}\}$ of all images dominated by A_μ or A_ν or both, (3) form each possible union of $*_\mu \cup *_\nu$ with the different combinations of the members of $\{*_{\kappa(1)}, \ldots, *_{\kappa(n)}\}$. The set of unions formed in step three is the excitation-equivalence class. The other way to form an excitation-equivalence class is to carry out steps (1)–(3) with a single A_μ, rather than a pair.

2.3. Lesions: Reducing the Set of Receptive Fields Even Further

The previous subsection described the limited ability of the paramedian lobule to discriminate stimulus arrays, compared to the anterior lobe. When receptive fields are eliminated by inhibition, injury, or the functional state of the circuit, ability to discriminate can be further degraded (Fig. 8). The degradation can be represented by increase in the size of excitation-equivalence classes or by one image coming to dominate another.

For example, if the receptive field including only toe 4 is eliminated, A_3 comes to dominate A_4. Then the two excitation-equivalence classes associ-

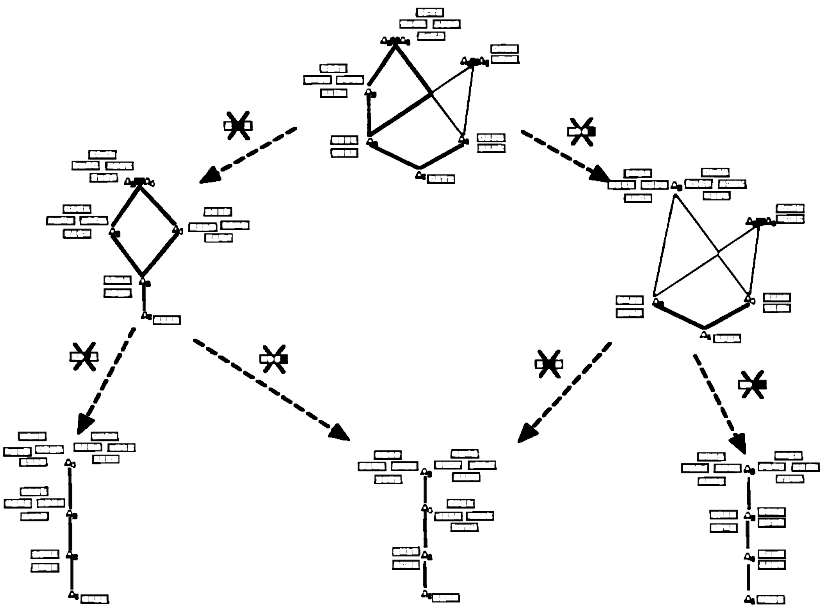

Fig. 8. Changes in excited ensembles and excitation-equivalence classes in the paramedian lobule as receptive fields are eliminated. This is a way to study the effects of lesions on the ability to discriminate stimulus arrays. At the center top is the poset from Fig. 7, with the largest number of excited ensembles and the largest number of excitation-equivalence classes. Dashed arrows lead to posets with smaller numbers of excited ensembles. By each dashed arrow is a diagram of the receptive field that is removed to reduce the excited ensemble poset. As each receptive field is removed, unions of images become equal to each other, collapsing excitation-equivalence classes together.

ated with A_3 and $A_3 \cup A_4$ are merged. Another way to think of it is that, in the excitation-equivalence class associated with A_3, $*_3$ was formerly taken in union with all possible combinations from $\{*_1, *_2\}$, but now $*_4$ is included in that set, making $\{*_1, *_2, *_4\}$.

After multiple receptive fields are eliminated, two images A_μ and A_ν may come to be equal. Then their associated excitation-equivalence class consists of all possible unions of one or both of $*_\mu$ and $*_\nu$ with combinations of the stimuli associated with single-compartment images dominated by A_μ $(=A_\nu)$.

2.4. Residuated Excitation

A more general statement can be made about the type of mapping from stimulus arrays to excitation that occurs in the cerebellum. This type of mapping will be compared to a different one in the next section; the two

types of mappings correspond to two major types of behavior observed in climbing fiber experiments.

Let $*_i$ be defined as above and S be the poset of stimulus arrays, even if the receptive fields do not obey the rules of combination found among the climbing fibers. Let the set of cells excited by a one-time stimulus $\cup *_{i \in I} *_i$ be the union of images $\cup_{i \in I} A_i$ of single compartments. Define a new set E to be the set of all cell ensembles D such that any two cells with the same receptive field either belong both to D or both to D (complement of D, that is, the set of all cell ensembles not in D). So E is the poset of all possible excited ensembles, where no distinction is made between cells with the same receptive field.

Let the map α: $S \rightarrow E$ take stimulus arrays onto their excited cell ensembles, so that

$$\alpha(\cup_{i \in I} *_i) = \cup_{i \in I} A_i$$

Elements of E of the form $\cup A_i$ are at the general case. Furthermore, there are distinct stimulus arrays in S that map onto the same element e of E, if there is a single-compartment image that is dominated by a union of other single-compartment images. The role of α is (1) to single out those elements of E that are ensembles of cells excited by a one-time stimulus array, and (2) to map distinct stimulus arrays onto the same element of E in case a single-compartment image is dominated by a union of other single-compartment images.

Under the order "inclusion," denoted here with $\geq$, the map α is isotone, because if $\cup_{i \in I} *_i \geq \cup_{j \in J} *_j$, then

$$\alpha(\cup_{i \in I} *_i) = \cup_{i \in I} A_i \geq \alpha(\cup_{i \in J} *_j) = \cup_{j \in J} A_j$$

Now consider a map in the reverse direction, β: $E \rightarrow S$, defined as follows. Given $e \in E$, let I be the set of compartments such that $i \in I \Leftrightarrow A_i \leq e$. Notice that means I is exactly the largest set such that $\cup_{i \in I} A_i \leq e$. Then let

$$\beta(e) = \cup_{i \in I} *_i$$

the largest stimulus array whose image is contained in e, this image being in fact the largest contained in e.

If $e_1 \geq e_2$, then any image contained in e_2 is contained in e_1. So β is isotone, like α.

Now consider the composition of the two maps α and β. Given a set I of compartments,

$$\beta \circ \alpha(\cup_{i\in I} *_i) = \beta(\cup_{i\in I} A_i)$$

$$= \cup_{j\in J} *_j, \quad \text{where } J \text{ is the largest index set with}$$

$$\cup_{j\in J} A_j \leq \cup_{i\in I} A_i \text{ (so } J \supset I)$$

$$\geq \cup_{i\in I} *_i$$

So $\beta \circ \alpha \geq id_s$, where id_s is the identity on S. Now, for any given $e \in E$

$$\alpha \circ \beta(e) = \alpha(\cup_{i\in I} *_i), \quad \text{where } I \text{ is the maximum index set such that } \cup_{i\in I} A_i \leq e$$

$$= \cup_{i\in I} A_i$$

$$\leq e$$

So $\alpha \circ \beta \leq id_E$.

The maps α and β are a residuated pair (Blyth and Janowitz, 1972), because each is isotone, $\beta \circ \alpha \geq id_s$ and $\alpha \circ \beta \leq id_E$. Then the map $\tau = \beta \circ \alpha$ is a closure map on S in the sense that $\tau = \tau \circ \tau \geq id_s$ (Blyth and Janowitz, 1972, Theorem 2.7) (Fig. 9). The closed elements induced in S by the closure map τ are the excitation-equivalence classes.

A residuated mapping can be thought of as grouping subsets of characteristics into a whole object, just as the smell of an orange, its taste, or its feel evokes an image of a whole orange in the mind. As the set of receptive fields is changed, the residuated mapping changes to group stimulus arrays into different equivalence classes (or objects, in the analogy to sensing an orange). In this way, lesions can be thought of as changing the set of perceptible objects, equivalence classes, or patterns of excitation. Finding the set of perceptible objects is an important practical problem in caring for neurological patients.

3. SEQUENTIAL STIMULI AND THE SUBTHRESHOLD OSCILLATION

The climbing fiber behavior considered in the previous section is consistent with much of the experimental literature, but does not yet display observed event detector behavior: responses only to unusual stimulation or unexpected events (Rushmer *et al.*, 1976; Gilbert and Thach, 1977; Gellman *et al.*, 1985). By taking into account sequential stimuli and subthreshold oscillation, this section shows that both rhythmic and event detector behavior are consistent with underlying rhythmic properties.

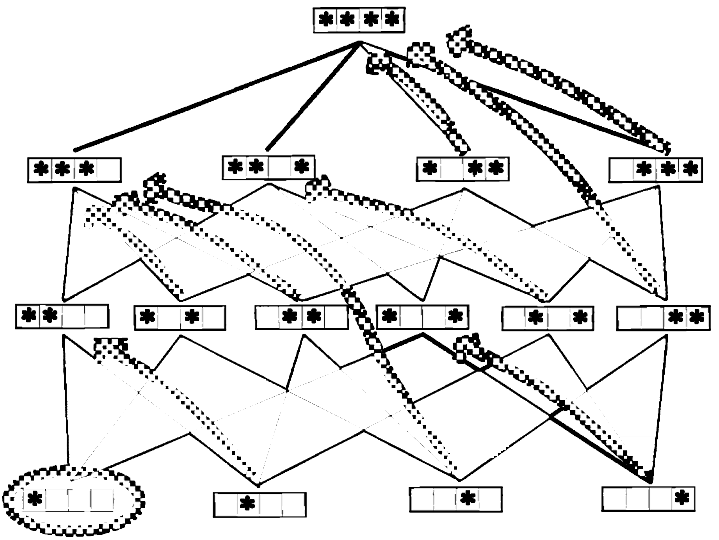

Fig. 9. Closure mapping $\beta \circ \alpha$ for toepad stimulus arrays and excitation in the paramedian lobule. Patterned arrows are superimposed on the poset S of stimulus arrays on four toepads. The patterned arrows lead from an element to its closure. Each excitation-equivalence class maps onto one closed element, its closure, in S.

The temporal relationship between the sequential stimulation and the subthreshold oscillation determines the type of mapping from stimulus to response, whether the mapping is residuated, as in the previous section, or whether the mapping describes behavior more like an event detector. As in the previous section, the stimuli may be tactile arrays rather than single-compartment stimuli. This section considers mappings that fall into both categories.

The physiological basis for rhythmic behavior in climbing fibers is the spontaneous oscillation of the olivary cell's membrane potential (Bell and Kawasaki, 1972; Llinás and Sasaki, 1989). The oscillation does not usually cause the cell to spike unless there is a stimulus, so it is called a "subthreshold oscillation." Stimuli set and reset the phase of the subthreshold oscillation, affecting the activity in response to subsequent stimuli (Llinás and Sasaki, 1989).

Because the interaction of stimuli with the subthreshold oscillation is of interest, the stimuli to be considered are restricted to temporally regular ones that repeat after a fixed number of beats. A stimulus sequence of period n will be specified by the notation $(:s_1:s_2: \ldots :s_n:)$ of stimulus arrays occurring in one cycle of the stimulus sequence, and by giving the beat-to-beat time d from the onset of one stimulus array (or beat) to the next as a fraction of the subthreshold oscillation period, or preferred period for activity. The period

is not defined to be the least number of repeating elements, but can be considered to be $2n$, $3n$, etc. In general, the delays may be inserted in the stimulus-delay sequence: $(:s_1:d_1:s_2:d_2: \ldots :s_n:d_n:)$. In this paper, the duration of the stimuli will be assumed to be insignificant compared to any d_i, $i = 1, \ldots, n$. Also, d_i will be taken to be the constant d throughout the sequence, so it can be omitted from the sequence and specified separately. Irregular rhythms may be denoted by inserting empty stimulus arrays so that, for example, the stimulus-delay sequence $(:s_1:1:s_2:2:)$ can be denoted as a pure stimulus sequence $(:s_1:s_2:\phi:)$ with $d = 1$. The stimulus sequences are considered to be infinite in both directions in time.

3.1. Mapping Types for One-Spike Responses

The previous section considered mappings α from stimulus to excitation. This section carries the mapping from excitation to response. Two stimuli may be response-equivalent simply because they are excitation-equivalent. This subsection considers only responses of one spike; later, the generalization to multiple-spike responses will be sketched.

First, the definition of the map α is generalized to sequences: each stimulus in $(:s_1:s_2: \ldots :s_n:)$ maps individually onto a union of single-compartment images:

$$\alpha(:s_1:s_2: \ldots :s_n:) = (:\cup_{k\in K(1)} A_k:\cup_{k\in K(2)} A_k: \ldots :\cup_{k\in K(n)} A_k:)$$

where the colon notation is also used for images and where the $K(i)$ are the appropriate sets of compartments.

Each stimulus resets the phase of the subthreshold oscillation by resetting the membrane potential to its most responsive (from which point it oscillates) (Llinás and Sasaki, 1989). Because of this, repeated excitation of an image evokes activity with a probability given by d (the delay given as a fraction of the preferred period). The probability p of a response is a function of d, approximately

$$p(d) = \frac{(1 + \cos 2\pi d)}{2}$$

although it may not be exactly a sinusoid (Llinás and Sasaki, 1989). So if $d = 1$, excitation of the image sequence evokes a one-spike response every time, whereas if $d = 1/2$, excitation of the image sequence never evokes any response. The clearest example of the phenomenon in the case $d = 1$ is for a sequence consisting of a single repeated one-compartment stimulus $(:*_i:)$:

$$\gamma \circ \alpha(:*_i:) = \gamma(:A_i:)$$
$$= \rangle:A_i:\langle$$

where γ maps from excitation to response and the ⟨angle⟩ brackets denote neural activity (also referred to as response or spiking). The activity interval is the same as the stimulus interval and the stimulated and active images are always the same for $d = 1$. However, if $d = 1/2$, there is no activity at all.

The difference between residuated and event detector behavior becomes more apparent when intersecting images are considered. If d is any integer, every excitation leads to a response:

$$\begin{aligned}\gamma \circ \alpha\,(:\cup_{k\in K(1)} *_k:\cup_{k\in K(2)} *_k: \ldots :\cup_{k\in K(n)} *_k:) \\ = \gamma(:\cup_{k\in K(1)} A_k:\cup_{k\in K(2)} A_k: \ldots :\cup_{k\in K(n)} A_k:) \\ = \rangle:\cup_{k\in K(1)} A_k:\cup_{k\in K(2)} A_k: \ldots :\cup_{k\in K(n)} A_k:\langle\end{aligned}$$

In contrast, when $d = 1/2$ (or another half-integer value), sets of cells with certain receptive fields are eliminated from the activity in an image, because they are repeatedly reset. Let B_r denote the set of climbing fibers with receptive field r. (Then the B_r are subsets of the A_i, and the set of all climbing fibers is the disjoint union over all of the B_r.) Writing $T(i)$ and $T(j)$ for the sets of receptive fields containing compartments i and j, respectively, we have

$$\gamma(:A_i:A_j:) = \rangle:\cup_{r\in T(i)} B_r - \cup_{r\in T(j)} B_r:\cup_{r\in T(j)} B_r - \cup_{r\in T(i)} B_r:\langle$$

where $a - s = a \cap \bar{s}$, since $A_i = \cup_{r\in T(i)} B_r$ and $A_j = \cup_{r\in T(j)} B_r$.

There are several reasons, specific to the inferior olive, to choose integer and half-integer intervals. First, the probability of firing is probably not exactly sinusoidal (Llinás and Sasaki, 1989). Stimuli falling on a peak or in a trough can be considered with reasonable confidence, but treatment of intermediate values is likely to be inaccurate. Another reason is that there is variability in preferred period within a cell population, so more numerical precision is perhaps not appropriate for images.

The behavior of the mapping in distinguishing between sequences can be envisioned by starting with the poset Q_n of doubly infinite sequences of excited ensembles that repeat after n elements, where inclusion is given by

$$(:X_1:X_2: \ldots :X_n:) \geq (:Y_1:Y_2: \ldots :Y_n:)$$

if $X_i \geq Y_i$ for every i, or if there is cyclic permutation such that there is element-by-element inclusion. The two-compartment stimuli, receptive fields, and excitable ensembles shown in Fig. 10 will serve as a basis for later examples. It can also cover inclusion between sequences of different numbers of elements if null excited ensembles are interposed; for example, $(:X_1:X_2:)$ with $d = 1$ can be written as $(:X_1:\phi:X_2:\phi:)$, and then

$$(:X_1:X_1:X_2:X_2:) \geq (:X_1:\phi:X_2:\phi:)$$

If networks of sequences are studied, a definition of aggregate inclusion may be required.

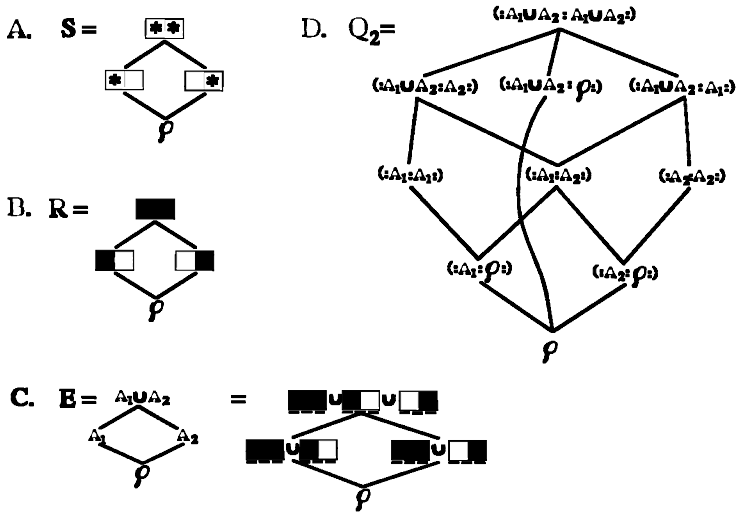

Fig. 10. Example of two compartments: stimulus arrays, receptive fields, excited ensembles, and excited ensemble sequences of period 2. (A) Stimulus array poset *S*. (B) Receptive field poset *R*. (C) Ensemble poset *E*. First it is drawn using the conventions of Fig. 6, and then writing the images as unions of ensembles, represented here by their receptive fields, with dashed underlining. (D) Poset Q_2 of two-element sequences of excited images. Each sequence is enclosed in parentheses. The elements of a sequence can appear in either order, because the sequence repeats. Q_2 is a lattice, but Q_n is not in general a lattice for $n > 2$.

The response evoked by exciting the sequences in Q_2 can be found by determining the interval between occurrences of each receptive field and multiplying the subsequent activity of the receptive field by the probability of firing (Fig. 11). Let $F_n(d)$ be the poset of sequences of active ensembles, denoted with loudspeaker brackets. [The relationship of $F_n(d)$ to Q_n depends on d, so it is specified in the notation.] For $d = 1$, the poset of activity patterns $F_2(1)$ is isomorphic to Q_2. However, for $d = 1/2$, $F_2(1/2)$ is smaller; more than one element of Q_2 maps onto the same element of $F_2(1/2)$, in particular, $(:A_1 \cup A_2 : A_1 \cup A_2 :)$, $(:A_1 : A_1 :)$, $(:A_2 : A_2 :)$, and ϕ all map onto ϕ (Fig. 12). Thus, the subthreshold oscillation introduces another type of response-equivalence, for sequences, besides the type of response-equivalence arising from excitation-equivalence described in the previous section, introduced by one image dominating another.

For half-integer d, the map γ can be specified in general by considering that when each element X_i of a sequence $(:X_1: \ldots :X_n:)$ is excited, the set of climbing fibers that are activated can be found by a series of subtractions. If the number n of elements in the cycle is odd, an element of the sequence of excitations resets the cells in its ensemble so that its own repetition hits a trough, whereas if n is even, an element of the sequence of excitations

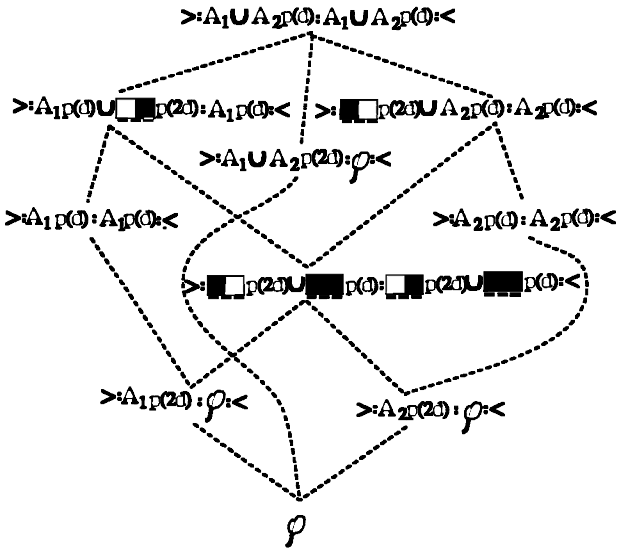

Fig. 11. Activity patterns $F_2(d)$ for arbitrary d, stimulated by the two-element sequences shown in Fig. 10D. Activity is enclosed in loudspeaker brackets. Images are multiplied by the probability of firing. Dashed lines indicate that inclusion is induced from Q_2.

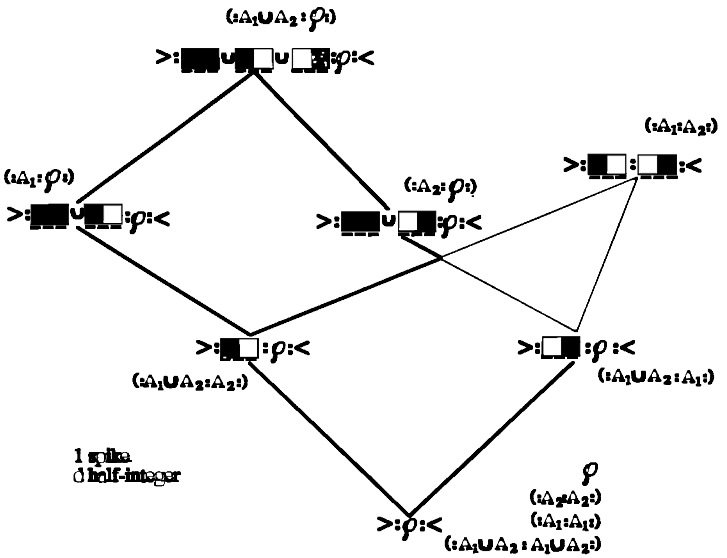

Fig. 12. Poset of activity sequences $F_2(1/2)$ evoked by the two-element sequences shown in Fig. 10D at a half-integer sequence interval with a one-spike response. Near each activity sequence in loudspeaker brackets is a list of the members of the response-equivalence class of sequences. The format is that of Fig. 7, except that the poset is of activity rather than excited images and the equivalence classes are of sequences rather than stimulus arrays.

resets the cells in its ensemble so that its own repetition hits a peak of the subthreshold oscillation. What fires in response to excitation of X_i is

$$X_i - [(X_k - (X_{k+1} \cup X_{k+3} \cup \ldots \cup X_{k+n-2})) \cup (X_{k+2} - (X_{k+3} \cup X_{k+5} \cup \ldots \cup X_{k+n-2})) \cup \ldots \cup (X_{k+n-3} - X_{k+n-2}) \cup X_{k+n-1}]$$

where $k = i$ for n odd and $k = i + 1$ for n even, because those are the first elements that must be subtracted in each case.

For $n = 3$, what fires in response to one stimulus in the sequence is

$$X_i - [(X_i - X_{i+1}) \cup X_{i+2}] = X_i \cap X_{i+1} \cap (\overline{X_{i+2}}) = (X_i \cap X_{i+1}) - X_{i+2}$$

Some special sequences are

$$\gamma(:a:a:a:) = \rangle:\phi:\langle$$
$$\gamma(:a:a:b:) = \rangle:a - b:\phi:\phi:\langle$$
$$\gamma(:a:a:\phi:) = \rangle:a:\phi:\phi:\langle$$
$$\gamma(:a:b:\phi:) = \rangle:a \cap b:\ \phi:\phi:\langle$$
$$\gamma(:a:\phi:\phi:) = \rangle:\phi:\langle$$

Response-equivalence arising from the subthreshold oscillation has been illustrated for $n = 2$, first in the case of general d (Fig. 11) and then as a poset of responses, showing which excitations map onto them for half-integer d (Fig. 12). The behavior of the entire mapping is clearer in the case of $n = 3$. Figure 13 shows the poset of excitations Q_3 over the two-compartment S and E shown in Figs. 10A and 10C. Figure 14 shows the response-equivalence classes that result from mapping Q_3 into $F_3(1/2)$, the poset of responses of length 3 for $d = 1/2$.

To show whether the mapping γ from excitation to response is residuated, a map from response back to excitation is required. Such a mapping can be thought of as displaying the information about the stimulus that the nervous system can find in its own response. The map γ takes the poset of excited ensemble sequences Q_n into the poset of activity sequences $F_n(d)$. Depending on the value of d, sequences in Q_n may be response-equivalent to each other. Let the map δ take the poset of activity sequences $F_n(d)$ back into the poset of excited ensembles Q_n, so that the composition $\delta \circ \gamma$ induces a map from Q_n to itself, analogous to the map $\beta \circ \alpha$ from S to itself. Like the map $\beta \circ \alpha$, the map $\delta \circ \gamma$ might not be injective. It will be constructed to map everything in a given response-equivalence class of Q_n onto the same element of Q_n. Unlike $\beta \circ \alpha$, $\delta \circ \gamma$ is not always a closure. As a pair, the maps α and β

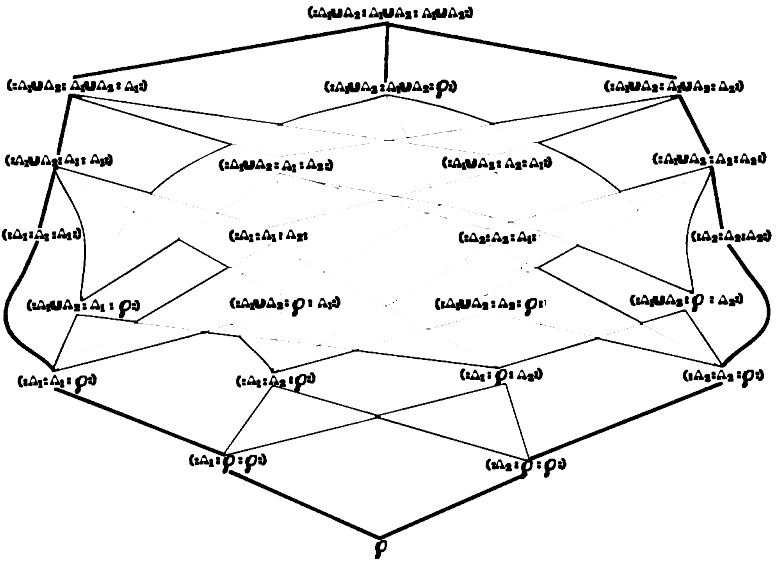

Fig. 13. Poset Q_3 of three-element sequences of excited images over the stimuli, receptive fields, and images shown in Figs. 10A–10C. Conventions as in Fig. 10D.

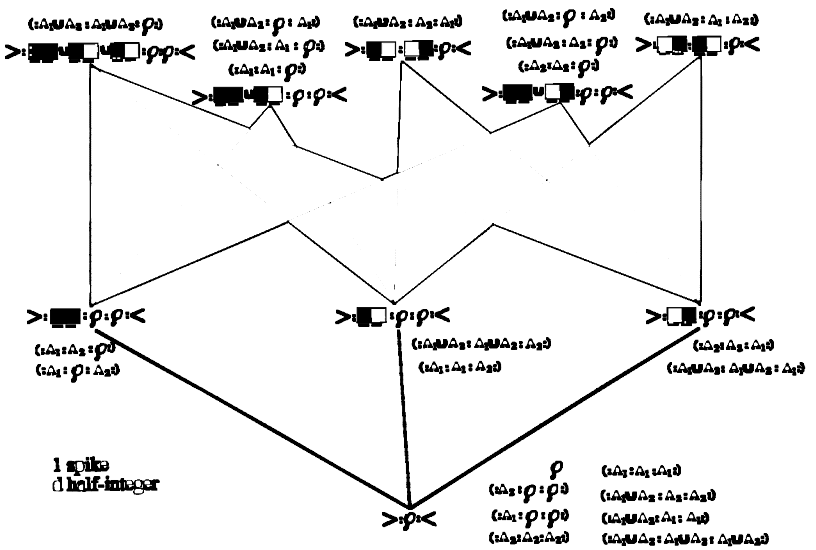

Fig. 14. Poset of activity sequences $F_3(1/2)$ evoked by the three-element sequences shown in Fig. 13 at a half-integer sequence interval. The response is one spike. Conventions as in Fig. 12.

allow a definition of excitation-equivalence. Similarly, the pair $\gamma \circ \alpha$ and $\beta \circ \delta$ allow a definition of response-equivalence.

Following the example of Fig. 14, there are many ways to construct a map $\delta \circ \gamma$: $Q_3 \rightarrow Q_3$ so that response-equivalence classes are mapped onto one of their own members in Q_3. However, such a map would not in general be a closure for half-integer d because, as shown in Fig. 15 , some response-equivalence classes contain elements that are not dominated by a common element in their response-equivalence class. Figure 15 exemplifies nonclosure maps arising from half-integer d as Fig. 9 exemplifies closure maps resulting from residuated pairs and arising in the purely spatial case and from sequential stimulation at integer d.

3.2. Multiple-Spike Responses

Response-equivalence can also result from a response consisting of multiple spikes (Llinás and Sasaki, 1989), because a continuing response may mask whether a later response has occurred.

Even though the responses may be different, in some cases the response-equivalence classes may be the same. For $d = 1/2$, the same set of equivalence classes occurs for Q_3 over the two-compartment S and E above when there is a one-spike response (Figs. 14 and 15) and when there is a two-spike response.

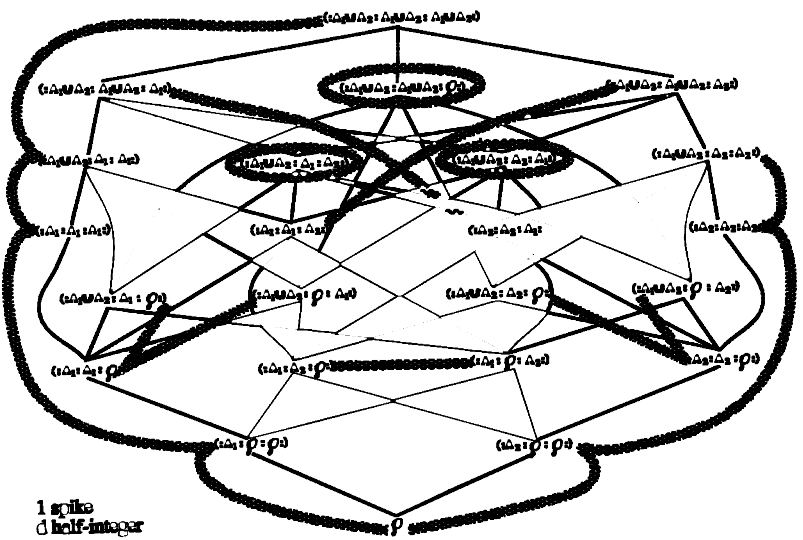

Fig. 15. Response-equivalent elements of Q_3 (Fig. 13) with half-integer d, showing the pattern of their occurrence in Q_3. Response-equivalent sequences are connected by broad lines with a wavy pattern. Sequences in ovals are singletons, not response-equivalent to other sequences.

It is tantalizing to think that more general results of this type might hold. Such a constancy of equivalence classes does not hold for even n and integer d.

Multiple spikes group responses, rather than leading to event detector behavior like that arising from stimulus sequences at half-integer intervals, as will be shown by finding closure maps. For integer d and one-spike responses, an arbitrary sequence maps as follows:

$$\gamma(:X_1: \ldots :X_n:) = \rangle:X_1: \ldots :X_n:\langle$$

For two-spike responses,

$$\gamma(:X_1: \ldots :X_n:) = \rangle:X_n \cup X_1:X_1 \cup X_2: \ldots :X_{n-1} \cup X_n:\langle$$

For three-spike responses,

$$\gamma(:X_1: \ldots :X_n:)$$

$$= \rangle:X_{n-1} \cup X_n \cup X_1: X_n \cup X_1 \cup X_2: \ldots : X_{n-2} \cup X_{n-1} \cup X_n: \langle$$

And so on, so that for m-spike responses the unions are over m elements.

For integer d and one-spike responses, it is natural to choose δ to map each activity sequence back onto its image sequence:

$$\delta(\rangle:X_1:X_2: \ldots :X_n:\langle) = (:X_1:X_2: \ldots :X_n:)$$

so that any two different excitation sequences are distinguishable as activity sequences. For integer d, but given two-spike responses, two excitation sequences are distinguishable in the resulting activity unless they contain successive triples such that

$$X_i \cap X_{i+2} \geq X_{i+1}$$

because the first spike from X_{i+1} will be masked by the second spike from X_i and the second spike from X_{i+1} will be masked by the first spike from X_{i+2}. If element X_{i+1} is masked, then the largest set $I = \{1, \ldots, n\}$ of single compartments such that the union of their images A_i, $i \in I$, could be in X_{i+1} is the largest set I such that

$$\cup_{i \in I} A_i \leq X_i \cap X_{i+2}$$

If two sequences are the same except for a masked X_{i+1} (and a cyclic permutation), then they are response-equivalent for two-spike responses, and they are both contained in the similar sequence containing the maximal $X_{i+1} = X_i \cap X_{i+2}$. Using the definition of δ for integer d, all the activity sequences are mapped by δ onto the sequence of images containing the maximal X_{i+1}. Then $\delta \circ \gamma$ is a closure, because $\delta \circ \gamma(:X_j:) \geq (:X_j:)$. Similar arguments can be used to show that $\delta \circ \gamma$ is a closure for integer d in circumstances in which responses consist of any fixed number of spikes.

4. DISCUSSION

This paper has addressed the ability of the nervous system to distinguish tactile stimuli by means of ensemble responses among cerebellar climbing fibers, on the basis of interpretations of receptive field data and physiological experiments. The principles, which are displayed in simple examples, apply equally to more complex receptive fields and stimuli, because the receptive fields are still generated according to simple rules. For example, although the neighbor sets on the paw are based on four compartments, the number of compartments in a line on the face can be much larger (Castelfranco *et al.*, 1994).

The results of this paper can be generalized to give the full structure of climbing fiber responses on various parts of the body. The various anatomical equivalence classes of the paws can be concatenated and then joined to the paw parts that do not fall into anatomical equivalence classes. Both on the face and on the paws, there are sets of CF-continguous compartments that do not fall simply into a line, but branch, leading to posets of a more general form. Along the toes, the anatomical equivalence classes themselves form a branched structure, with two branches meeting to form a cycle of toe CF-contiguity, so the isomorphic triangular subposets in the poset of paw receptive fields do not themselves form a triangle (McCollum, 1992).

Similarly, the results of this paper can be generalized to various vertebrate species. Other species have different forms of receptive fields (Robertson and Laxer, 1981; Logan and Robertson, 1986), but the cerebellar physiology and therefore the mappings described in this paper are the same (Bloedel and Courville, 1981).

The methods used in this study allow analysis of the consequences of eliminating receptive fields, such as by inhibition, injury, or the functional state of the circuit. Also, fewer stimulus arrays and fewer sequences of stimulus arrays can be distinguished, in general, when more images are dominated by other images (as in the paramedian lobule), when the response consists of more spikes, and when the stimuli in the sequence are separated by an interval $d = 1/2$, half the period of the subthreshold oscillation.

Not only does distinguishability vary, but also the set of response ensembles varies with the image poset, the sequence interval d, and the number of spikes in the response. Perhaps the nervous system's primary task is to use the set of response ensembles to determine the conditions under which it was produced.

Furthermore, the type of mapping used in distinguishing response-equivalence classes varies. For distinguishing excited images, the map $\beta \circ \alpha$ is a closure. For integer d, $\delta \circ \gamma$ is a closure. A closure maps a set of stimuli (or excitations) onto a set that includes it, as in smelling an orange and being reminded of its taste, color, and texture: any subset of stimuli call up the whole set.

For half-integer d, the examples shown are not closures, and it seems that such maps would seldom be closures. For half-integer d, the tendency of the maps to allow only changes in excitation to be expressed in neural activity is reminiscent of the suggestions that the climbing fibers act as event-detectors (Rushmer *et al.*, 1976), training signals (Houk, 1989), or exploratory mechanisms (Bower and Kassel, 1990).

There are many way the nervous system could exploit the properties of these maps. One way would be to plan movements so that the stimuli always arrive on the peak of the subthreshold oscillation. Then ensemble activity characteristic of half-integer d would be the domain of unfamiliar movements or unpredicted environmental phenomena. Another way to exploit the properties of these maps would be to plan movements to receive stimuli on the peak of the subthreshold oscillation, but to cancel their response by resetting the climbing fibers with another signal, either internal to the nervous system or from a cleverly planned other sensory source. Similar effects might be observed, and exploited by the nervous system, in any cell population with a refractory period or an inherent oscillation.

ACKNOWLEDGMENTS

I am indebted to Richard J. Greechie for insisting, draft after draft, that the paper could be clearer; clarity of presentation has aided clarity of thought. Jan Holly has contributed a major editing job; she has not only cleaned up details, but helped me think through what I really meant. Ann M. Castelfranco helped bridge the gap from neurophysiology to mathematics in early drafts. Lee T. Robertson not only helped edit, but has taught me a great deal over our years of collaboration. John I. Simpson has both given information and discussed the observations in a thought-provoking way. A reviewer has contributed detailed, thoughtful questions. Patrick Roberts taught me the significance of the word "mechanism" to biologists and made the point that phase-locking is not a completely continuous phenomenon. Phoebe Caner offered hospitality during the writing of the very first draft. The research has been supported by NIH grants RO1-NS23209→DC02482.

REFERENCES

Bell, C. C., and Kawasaki, T. (1972). Relations among climbing fiber responses of nearby Purkinje cells, *Journal of Neurophysiology*, **35**, 155–169.

Bloedel, J. R., and Courville, J. (1981). A review of cerebellar afferent systems, in *Handbook of Physiology*, V. B. Brooks, ed., American Physiological Society, Bethesda, Maryland, pp. 735–829.

Blyth, T. S., and Janowitz, M. F. (1972). *Residuation Theory*, Pergamon Press, Oxford.

Bower, J. M., and Kassel, J. (1990). Variability in tactile projection patterns to cerebellar folia Crus IIA of the Norway rat, *Journal of Comparative Neurology*, **302**, 768–778.

Castelfranco, A. M., Robertson, L. T., and McCollum, G. (1994). Detail, proportion, and foci among face receptive fields of climbing fiber responses in the cat cerebellum, *Somatosensory and Motor Research*, **11**, 27–46.

Gellman, R., Gibson, A. R., and Houk, J. C. (1985). Inferior olivary neurons in the awake cat: Detection of contact and passive body displacement, *Journal of Neurophysiology*, **54**, 40–60.

Gilbert, P. F. C., and Thach, W. T. (1977). Purkinje cell activity during motor learning, *Brain Research*, **128**, 309–328.

Houk, J. C. (1989). Cooperative control of limb movements by the motor cortex, brainstem, and cerebellum, in *Models of Brain Function*, R. M. J. Cotterill, ed., Cambridge University Press, Cambridge.

Llinás, R., and Sasaki, K. (1989). The functional organization of the olivo-cerebellar system as examined by multiple Purkinje cell recordings, *European Journal of Neuroscience*, **1**, 587–602.

Logan, K., and Robertson, L. T. (1986). Somatosensory representation of the cerebellar climbing fiber system in the rat, *Brain Research*, **372**, 290–300.

McCollum, G., and Robertson, L. T. (1988). Patterns of intersection among climbing fiber receptive fields, *Neuroscience* **27**, 93–105.

McCollum, G. (1992). Rules of combination that generate climbing fiber tactile receptive fields, *Neuroscience* , **50**, 707–725.

McIlwain, J. T. (1986). Point images in the visual system: New interest in an old idea, *Trends in Neuroscience* **9**, 354–358.

Robertson, L. T. (1987). Organization of climbing fiber representation in the anterior lobe, in *New Concepts in Cerebellar Neurobiology*, J. S. King, ed., Liss, New York, pp. 281–320.

Robertson, L. T., and Elias, S. A. (1988). Representations of the body surface by climbing fiber responses in the dorsal paraflocculus of the cat, *Brain Research*, **452**, 97–104.

Robertson, L. T., and McCollum, G. (1989). Ensembles of climbing fiber tactile receptive fields encode distinct information for various cerebellar regions, in *The Olivocerebellar System in Motor Control*, P. Strata, ed., Springer-Verlag, Berlin, pp. 237–241.

Robertson, L. T., and McCollum, G. (1991). Stimulus classification by ensembles of climbing fiber receptive fields, *Trends in Neuroscience*, **14**, 248–254.

Robertson, L. T., and Laxer, K. D. (1981). Localization of cutaneously elicited climbing fiber responses in lobule V of the monkey cerebellum, *Brain, Behavior and Evolution*, **18**, 157–168.

Rushmer, D. S., Roberts, W. J., and Augter, G. K. (1976). Climbing fiber responses of cerebellar Purkinje cells to passive movement of the cat forepaw, *Brain Research*, **106**, 1–20.

Rushmer, D. S., Woollacott, M. H., Robertson, L. T., and Laxer, K. D. (1980). Somatotopic organization of climbing fiber projections from low threshold cutaneous afferents to pars intermedia of cerebellar cortex in the cat, *Brain Research*, **181**, 17–30.

Schwartz, E. L. (1977). Spatial mapping in the primate sensory projection: Analytic structure and relevance to perception, *Biological Cybernetics*, **25**, 181–194.

Simpson, J. I., Wylie, D. R., and De Zeeuw, C. I. (1996). On climbing fiber signals and their consequence(s), *Behavioral and Brain Sciences* **19**, 380–394.